CrossMark

Effect of functionalized CNTs and liquid crystalline polymer on thermo-oxidative stability of polyethylene-based hybrid composites

Supattra Tangtubtim[1] · Sunan Saikrasun[2]

Abstract Hybrid composites based on polyethylene (PE) filled with thermotropic liquid crystalline polymer (LCP) and pristine or hydroxyl- or carboxylic-functionalized CNTs were prepared using melt extrusion process. Thermo-oxidative decomposition under dynamic and isothermal conditions was investigated using thermogravimetric analysis (TG). From TG profiles and activation energy analysis, the highest thermo-oxidative stability revealed from both dynamic and isothermal investigations was clearly observed for the PE-based hybrid composite filled with LCP and small amount of carboxylic-functionalized CNT. The melt rheological investigation showed that the effect of LCP and CNTs loading on viscoelastic characteristics of the composites was clearly pronounced at low frequency and the viscous part was found as a dominant factor. Complex viscosity, storage and loss moduli of the hybrid composite containing carboxylic-functionalized CNT showed the highest values compared among all samples examined. The morphological results observed using scanning electron microscopy and transmission electron microscopy indicated the improved dispersion of both LCP and carboxylic-functionalized CNT fillers. The obtained results indicated the importance of LCP-assisted dispersion of carboxylic-functionalized CNT through interface interaction, resulting in the remarkable improvement in thermo-oxidative stability of the composite.

Keywords Hybrid composite · Polyethylene · Carbon nanotube · Liquid crystalline polymer · Thermal stability · Rheology

Introduction

The massive utilization of polymer materials in our every day life is driven by their remarkable combination of properties, low mass and ease of processing. However, due to a relatively low thermal stability compared with metals or ceramics, improvement in the heat stability of polymers is therefore a major challenge for extending their applications. Over the past several decades, blending of commodity polymers with thermotropic liquid crystalline polymer (LCP) has been known to exhibit excellent mechanical properties, thermal endurance, chemical stability and low melt viscosity [1, 2]. Due to the rigid rod-like molecules of LCP, it can be preferentially aligned to form microfibrils under elongational or shear forces during melt processing and in situ reinforces the polymer matrix after cooling down. This type of the blend is called in situ composite [3]. Moreover, LCP can act as the processing lubricant by lowering the melt viscosity of blend system. In this regard, many research works have been extensively performed to date in order to substitute the conventional thermoplastics and to widely develop commercial applications of LCP or its composites [4–6]. However, the practical application of LCP is limited for use as a polymer matrix compared with conventional thermoplastic polymers because LCP is relatively expensive.

✉ Sunan Saikrasun
sunan.s@msu.ac.th

[1] Department of Chemistry, Faculty of Science, Buriram Rajabhat University, Buriram 31000, Thailand

[2] Creative Chemistry Research Unit, Department of Chemistry and Center of Excellence for Innovation in Chemistry, Faculty of Science, Mahasarakham University, Mahasarakham 44150, Thailand

During the past few decades, the investigations on polymer-based nanocomposites have been extensively interested to find their promising alternatives to traditional composites because of their ability to display synergistically advanced characteristics with small amounts of nanofiller. The typical improved properties include barrier properties, flame retardation, thermal stability, chemical and dimensional stabilities and mechanical properties when compared with their micro- and macrocomposite counterparts and their neat polymer matrices [7–9]. Carbon nanotubes (CNTs) are one of the interesting nanofillers which can potentially be used in many applications ranging from macroscopic material composites down to nanodevices. This material has excellent electronic properties, thermal conductivity and mechanical strength. In terms of thermal stability, CNT/polymer composites also have attracted a great deal of attention from polymer scientists because CNTs have very high thermal stability [10–12]. Most of the previous studies have suggested that both promoting and hindering effects of CNTs on the thermal stability of polymer are found. Moreover, the structures of the polymer matrix and the interaction between CNTs and the matrix have been found as the key factors for the thermal degradation behavior of CNT-filled polymer composites. However, CNT generally tends to bundle together and to form some agglomeration due to the intrinsic van der Waals attraction between the individual tubes. The functionalization of CNT as an effective method to achieve the uniform dispersion and their compatibility with polymer matrix can lead to the improvement of overall properties of the composites [13–15]. In case of olefinic matrices like polyethylene or polypropylene, the melt mixing with CNT generally leads to poor state of CNT dispersion due to a lack of compatibility. Therefore, to achieve a suitable state of CNT dispersion, different approaches are described in the literature [16–20]. A commonly used method is the application of maleic anhydride grafted PE or PP types to form the covalent bond to the CNT surface [21–24]. Recently, Müller et al. [16] investigated the dispersion of CNTs into polyethylene by an additive-assisted one-step melt mixing method. The main results showed the improved CNT dispersion with additive loading.

Recently, Kim et al. [25] investigated the effect of modified CNT on physical properties of LCP-based nanocomposites. They found that the incorporation of CNT plays a crucial role in improving the thermal stability by acting as effective physical barriers against the thermal decomposition in the LCP nanocomposites. Moreover, the mechanical properties of the nanocomposites were enhanced resulting from the synergistic effect combining good interfacial adhesion and uniform dispersion of CNT. This feature has motivated our affords to utilize CNT and LCP as the hybrid fillers for advanced composite materials with the realized benefit of practical application in industrial field such as electronic and electric appliances. The presence of LCP interfacial bonded with CNT is expected to reduce agglomeration CNT. Under conventional melt mixing, the enhanced dispersion state of CNT is expected to achieve by LCP-assisted dispersion of CNT. Thereby, the improved physical properties of the composite materials can be expected. However, the suitable functionalized CNTs are one of the main factors affecting the interaction with LCP phase.

The main objective of this work is to improve the thermo-oxidative stability of high-density PE by modifications with CNTs and LCP under composite preparation using common extrusion process. The well-dispersed LCP domains will be expected to interact with appropriate functionalized CNTs and function as the filler-assisted dispersion of CNTs or can be helpful in achieving the better dispersion state of CNTs. The improved dispersion of CNTs is expected to level up the thermo-oxidative stability of the composite materials. However, to improve the dispersion of CNTs, good interfacial bonding between LCP and appropriate functionalized CNTs is required. In this study, the hybrid composites based on high-density PE filled with LCP and different functionalized multiwall CNTs (pristine, hydroxyl- and carboxylic-functionalized CNTs) were prepared. The thermo-oxidative stability of all composites and the neat polymer matrix was investigated and compared.

Experimental

Materials

High-density PE grade 5000S with a melt flow index (MFI) of 0.80 g 10^{-1} min^{-1} was purchased from Bangkok Polyethylene (Thailand). The nanofillers used in the present work were pristine, hydroxyl- and carboxylic-functionalized multiwall CNTs purchased from Chengdu Organic Chemicals Co., Ltd. (China). The hydroxyl- and carboxylic-functionalized multiwall CNTs have a functionalized content of 1.76 and 1.23 mass%, respectively. Bulk density, outer diameter, length, specific surface area and purity of all types of CNTs were reported to be 0.28 g cm^{-3}, 20–30 nm, 20–30 mm, >110 m^2 g^{-1} and >95%, respectively. Thermotropic liquid crystalline polymer (LCP), a microfiller, used in this work was Rodrun LC3000, supplied by Unitika Co. Rodrun LC3000 is a copolyester of 60 mol% p-hydroxy benzoic acid (HBA) and 40 mol% PET with a melting point of 220 °C and a density of 1.41 g cm^{-3}. The molecular mass for LCP was not obtainable, since no solvent was found to dissolve Rodrun LC3000.

Preparation of composites

The polyethylene-based composites containing various compositions of LCP and CNTs were prepared by melt extrusion using a single-screw extruder (Haake Rheomex, Thermo Electron (Karlsruhe) GmbH, Karlsruhe, Germany), with a screw diameter of 16 mm, length-to-diameter (L/D) ratio of 25, a die diameter of 2 mm and a screw speed of 100 rpm. The temperature profiles for the preparation of the PE-based composites were 190–225 °C. The temperature profiles shown here represent the temperatures at hopper zone, two barrel zones and heating zone in the die head, respectively. The extruded strand was immediately quenched in a water bath, palletized and subsequently dried in a vacuum oven. The sample codes of each sample were designated as shown in Table 1. The composition of CNTs and LCP fillers was fixed at 1 and 10 mass%, respectively.

Thermo-oxidative decomposition analysis

Thermo-oxidative decomposition behavior was investigated using simultaneous TG and DSC measurements (TA Instruments SDT Q600, Luken's drive, New Castle, DE). The neat matrix and its composite samples of 8–10 mg were loaded in alumina crucible and then nonisothermally heated from ambient temperature to 700 °C at various heating rates. The measurement was taken in air with the flow rate of 100 mL min^{-1}. The TG and DSC data were simultaneously recorded online in TA Instrument's Q series Explorer software. The analyses of simultaneous TG and DSC data were done using TA Instrument's Universal Analysis 2000 software (version 3.3B).

The isothermal tests were performed at 320, 320, 340 and 360 °C for 100 min. The sample was heated at a rate of 20 °C min^{-1} from ambient temperature to the selected temperature of isothermal degradation. As soon as the system reached the selected temperature, the variations in sample mass with times were registered. The isothermal experiments were performed in air at a flow rate of 100 mL min^{-1}. The analyses of isothermal TG data were carried out using the same software as those of the non-isothermal investigation.

Table 1 Designations of the composites

Composite	Ratio of composition/mass%	Designation
LCP/PE	10/90	C1
CNT/PE	1/99	C2
LCP/CNT/PE	10/1/89	HC1
LCP/HO-CNT/PE	10/1/89	HC2
LCP/CNT-COOH/PE	10/1/89	HC3

Melt viscosity measurements

Rheological behavior in the molten state for PE and its composites containing CNTs and LCP was characterized with a plate-and-plate rheometer (Physica Anton Paar, MCR5000; Physica Messtechnik GmbH, Germany). The pellet samples were compression molded at 160 °C into a sheet of about 1.5 mm thick. The sheet was then punched into a disk 25 mm in diameter. The complex viscosity (η^*), storage (G') and loss (G'') moduli of all specimens were measured in the oscillatory shear mode with the strain amplitude of 5% within the angular frequency (ω) ranging from 0.6 to 500 rad s^{-1}. The measuring temperature was set at 165 °C. The gap between the two plates was set at 0.9 mm.

Morphological characterization

The fracture surfaces for the different composite strands were observed under the scanning electron microscope (SEM) (Jeol; JSM-6460LV, Tokyo, Japan) operated with an accelerating voltage of 15 kV. Prior to examination, the extruded strands were immersed in liquid nitrogen for 30 min and fractured. The specimens were sputter-coated with gold for enhanced surface conductivity. To investigate the dispersion state of CNTs, a transmission electron microscope (TEM, Techni 20, Phillips, Holland) was used. Ultrathin sections with a thickness of about 200–300 nm were cut from extruded strands using Leica Ultracut R (Leica Microsystems Gmbh, Germany).

Results and discussion

Nonisothermal decomposition behavior

The effects of LCP and different functionalizations of CNT on thermo-oxidative decomposition behavior of PE-based thermoplastic composites revealed by dynamic TG profiles are shown in Fig. 1. It is seen that TG curves of all samples remarkably reveal the different profiles. For the neat PE, the TG curve reveals at least two steps of mass loss at a temperature range of around 250–550 °C. The degradation mechanism of PE normally begins at the weak link site along the polymer chain once the thermally induced scission has occurred. The reaction of PE is responsible for the propene product, and the other gives rise to 1-hexene [26]. The addition of the LCP and/or CNT into the PE matrix clearly improves the thermo-oxidative stability of the matrix. This is due to the good inherent thermal stability of the fillers. It is generally known that the CNT filler has been known to possess excellent thermal conductivity. Therefore, the improvement in thermal stability of the
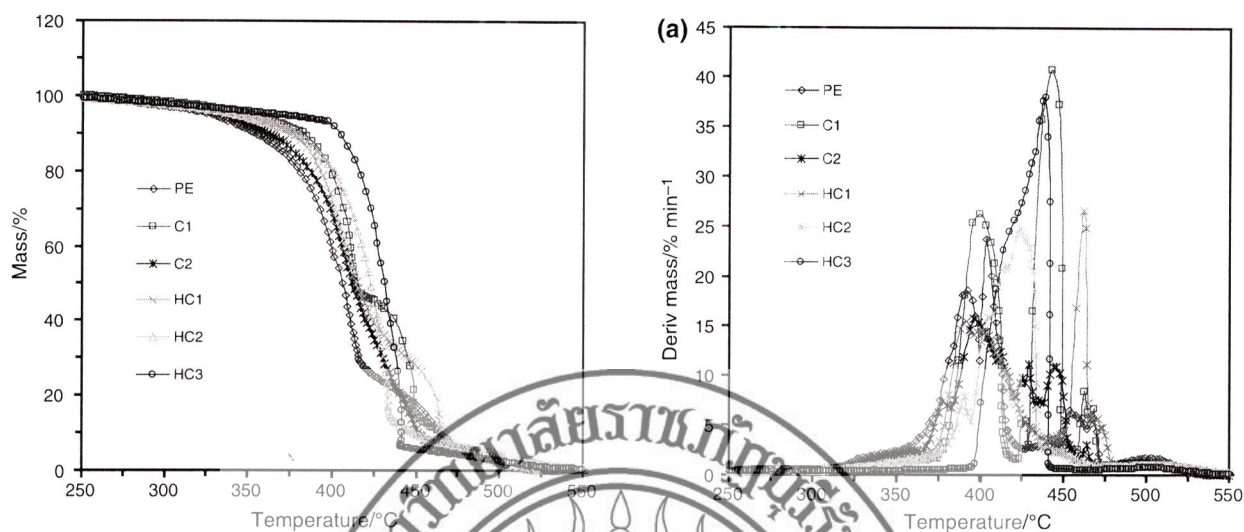
Fig. 1 Dynamic TG curves of PE, C1, C2, HC1, HC2 and HC3 at a heating rate of 10 °C min^{-1} in air

composites is also attributable to the formation and stabilization of CNTs-bonded macroradicals [27]. The stabilization effect of CNT was explained by the barrier effect of the nanotubes and their formed aggregates, which hinder the diffusion of the degradation product from the bulk of the polymer onto the gas phase. The increased thermal stability of CNT-containing composites over that of the neat matrix polymer is likely the result of adsorption, by activated CNTs surface, of free radicals generated during polymer decomposition. In case of C1, HC1 and HC2, the TG profiles show similar degradation behavior under heating from ambient temperature to 365 °C. The obtained results indicate that the presence of pristine and hydroxyl-functionalized CNTs slightly affects the thermo-oxidative stability of the composites. This may be due to that the adhesion between LCP and pristine or hydroxyl-functionalized CNTs is not good enough, hence resulting in poor dispersion state of the CNTs. Interestingly, the highest thermo-oxidative stability is observed for the hybrid composite of carboxylic-functionalized CNT system (HC3). The DTG profiles shown in Fig. 2 suggest complex reaction for the composites. As seen from Fig. 2a, most samples exhibit multi-DTG peaks during degradation due to complex decomposition behavior. For instance, C1 and HC1 exhibit the second major mass loss stages at around 440 °C which mainly involves the degradation of PET block of LCP [8]. The DTG peak of CNT, normally appeared at about 600 °C [8], is not clearly observed for the hybrid composites due to the use of small amount of CNTs. For C2 composite, the presence of pristine CNT alone also affects the degradation mechanism of PE [26] as clearly seen from the appearance of several small DTG peaks at 425–475 °C in comparison with decomposition

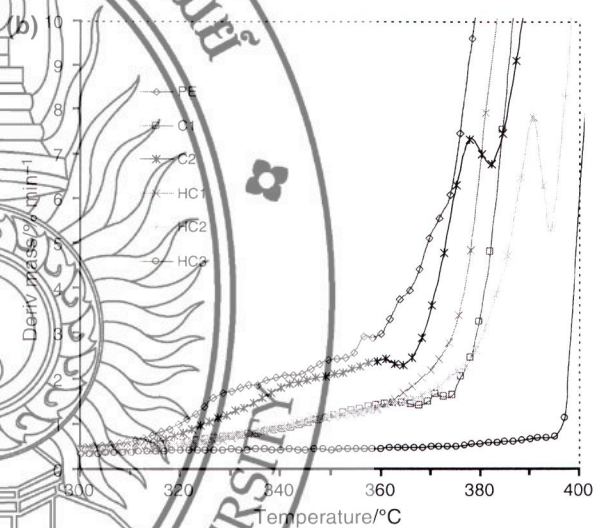**Fig. 2** DTG (a) and expanded DTG (b) curves of PE, C1, C2, HC1, HC2 and HC3 at a heating rate of 10 °C min^{-1} in air

behavior of the neat PE. Interestingly, HC2 and HC3 seem to exhibit major DTG peaks at around 424 and 437 °C, respectively. Beyond the major stage of the degradation, the DTG peak for HC2 and HC3 is not clearly observed. The obtained results indicated that the mass loss stages of the polymers change with filler loading and functionalized groups on CNT surface. To clearly compare the decomposition rate around the initial stage of degradation after the moisture has been evaporated, the DTG curves were expanded as shown in Fig. 2b. Under heating from ambient temperature to 300 °C, the decomposition rates of all samples are nearly the same and lie in a small narrow range of 0.1–0.4% min^{-1}. At higher temperature, the decomposition rate of PE firstly changes at ~310 °C followed by C2 (~315 °C), C1 or HC1 or HC2 (~320 °C) and HC3

($\sim$395 °C), respectively. In case of HC3, the thermo-oxidative resistance is significantly improved as seen from a maintainable constant value of decomposition rate which is prolonged up to $\sim$395 °C. Moreover, the thermo-oxidative resistance for C1, HC1 and HC2 revealed from the DTG curves is nearly the same and higher than those of C2 and PE.

Table 2 shows the summarized data of thermo-oxidative decomposition for the neat matrix and its composites. T_{onset} represents the onset degradation temperature. T_{max} represents the temperature at the maximum mass loss rate, $(d\alpha/dt)_{max}$. The subscripts 1, 2 and 3 represent the first, second and third stage of the degradation, respectively. It is seen that T_{onset} and T_{max1} values of HC3 are higher than those of other samples. The results suggest the improved thermo-oxidative stability for the hybrid composites containing carboxylic-functionalized CNTs. Moreover, the significant improvement in thermo-oxidative stability is dependent on both LCP and suitable functionalized CNT. This means that good filler–filler interaction occurs by forming hydrogen between carbonyl groups of LCP and carboxylic groups functionalized on CNT surface [25]. Therefore, the dispersion of the nanotube would be improved by LCP assisted CNT dispersion. Actually, CNTs are sheets of graphite rolled into tubes and have excellent properties due to their symmetric structure. Generally, the functional groups are grafted onto the defects of multiwall CNT generated at the broken penta-basic, heptatomic ring or at the open ends of multiwall CNTs. However, with the time prolonging or the temperature increasing, more rings around the defects would be broken; finally, the nanotube would be cut shorter, hence lowering the stability. Therefore, the presence of carboxylic functional groups onto the defects of CNT, which can form hydrogen bonding well with LCP, would effectively prolong the stability at higher temperature.

The simultaneous DSC traces of thermo-oxidative degradation for the neat PE and its composites are shown in Fig. 3. The corresponding peak temperature (T_d) and

enthalpy (ΔH_d) associated with the major degradation stage of all materials are also presented in Table 2. Melting temperature (T_m) of PE slightly decreases with fillers loading. The exothermic degradation process is observed for all the samples due to the fact that the concurrent and further degradation mechanisms in air tend to involve the formation reaction. PE shows a very broad degradation exotherm that stretches from 250 to 550 °C with a peak maximum (T_d) at $\sim$400 °C. Beyond this region, the remaining signal of PE is unstable as evident by the appearance of several minor peaks at 430–550 °C. It is seen that the minor DSC peaks for PE degradation are also observed for C1, C2 and HC1 composites at 425–530 °C. It is interesting to note that the minor peaks are diminished and disappeared for HC2 and HC3, respectively. This may be due to that the interaction between the two fillers would occur for the later two samples (HC2 and HC3), resulting in the improved dispersion state of CNTs. The better dispersed CNT filler is expected to effectively retard not only the major stage but also the minor stage of decomposition. The dispersion of the fillers for all composites will be shown and discussed in the section of morphology. Note that the enthalpy of thermal decomposition of PE and C2 shows the highest value (11.2 kJ mol^{-1}), whereas the enthalpy of HC3 sample shows the lowest value of (7.33 kJ mol^{-1}).

Isothermal decomposition behavior

Investigation of isothermal degradation is also complementary and necessary to get a complete description of the kinetics of thermo-oxidative decomposition process. The mass losses of the neat polymer and its composites were isothermally analyzed in air at four isothermal temperatures of 300, 320, 340 and 360 °C. The isothermal TG curves are presented in Fig. 4. The shapes of the isothermal TG profile for each sample strongly depend on temperatures and fillers. Under isothermal test at 300, 320 and 340 °C, the neat PE and C2 exhibit more rapid

Table 2 Dynamic TG and simultaneous DSC data of thermo-oxidative decomposition for PE and its composites at a heating rate of 10 °C min^{-1} in air

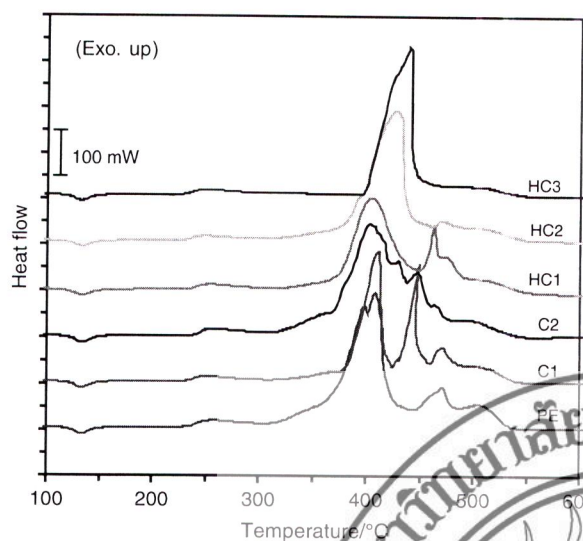| Sample	Dynamic TG data								Simultaneous DSC data			
	$T_{onset}/$ °C	$T_{max1}/$ °C	$(d\alpha/dt)_{max1}/\%$ min^{-1}	$T_{max2}/$ °C	$(d\alpha/dt)_{max2}/\%$ min^{-1}	$T_{max3}/$ °C	$(d\alpha/dt)_{max3}/\%$ min^{-1}	Char yield at 600 °C/%	$T_m/$ °C	$\Delta H_m/$ kJ g^{-1}	$T_d/$ °C	$\Delta H_d/$ kJ g^{-1}
PE	376	396	18.6	406	23.5	462	26.6	0	136	0.20	406	11.2
C1	399	400	26.3	442	40.8	462	8.31	0	135	0.17	410	8.73
C2	380	398	15.7	429	11.2	446	10.8	0	135	0.18	406	11.2
HC1	382	391	15.5	402	14.4	453	6.09	0	135	0.17	406	9.13
HC2	405	390	7.81	425	24.5	–	–	0.27	134	0.16	426	9.40
HC3	412	437	36.6	–	–	–	–	0.07	134	0.16	439	7.33

Fig. 3 Simultaneous DSC curves of thermo-oxidative decomposition for PE, C1, C2, HC1, HC2 and HC3 at a heating rate of 10 °C min^{-1} in air

contribution of these steps to the overall degradation rate changes with both temperature and extent of reaction. This means that the effective activation energies determined from thermal analysis data alone are not capable of revealing this type of reaction complexity. Therefore, to avoid the need to know decomposition mechanism required for some model fitting, a model-free approach is widely used for kinetic analysis. In this work, the reliable isoconversional method, namely Flynn–Wall–Ozawa (F–W–O) method [28, 29], was applied in order to quantitatively evaluate the thermo-oxidative stability of polymers under nonisothermal test. F–W–O is a relatively simple method which allows for evaluating kinetic parameters without choosing the reaction model. The activation energy of decomposition can be directly determined from mass loss versus temperature data obtained at several heating rates. This method is expressed by the following equation:

$$\ln \beta = \left[\frac{AE_a}{Rg(\alpha)} \right] - 5.3305 - 1.0516 \frac{E_a}{RT} \tag{1}$$

where β is a heating rate in °C min^{-1}, A is a pre-exponential factor, E_a is an activation energy (kJ mol^{-1}), T is an absolute temperature (K), R is an universal gas constant (J K^{-1} mol^{-1}), and $g(\alpha)$ is an integral reaction type of kinetic function. Normally, E_a value calculated by the isoconversional methods is called apparent activation energy because it is the sum value of activation energies of the chemical and physical decomposition processes. Figure 5 shows the effect of heating rates on TG profile (Fig. 5a) and the isoconversional plots as a function of mass loss using F–W–O method for C1 sample (Fig. 5b). From Fig. 5a, the shift of the TG curves to the higher temperature with increasing heating rate could be attributed to the short time required for a sample to reach a given temperature at the high heating rate [30]. The E_a values at various mass losses calculated from the isoconversional plots for the selected samples are presented in Table 4. It is seen that the E_a value of each sample mostly increases with mass loss, indicating that the degradation mechanism varies with the mass loss. As clearly observed from E_a values, the HC3 exhibits the highest thermo-oxidative stability under dynamic heating.

decomposition under heating for the first 20 min. Moreover, the isothermal stability of HC3 and C1 is nearly the same and shows the highest stability compared among all samples examined. Upon heating at 360 °C, it is interesting to note that a slow decomposition is clearly observed for HC3, whereas the all other samples rapidly degrade. This indicates the highest isothermal stability of HC3 similar to the results obtained from the nonisothermal investigation. Table 3 shows the isothermal decomposition data of the neat PE and its composites containing different fillers in air. t_{max} represents the time at maximum mass loss rate, $(d\alpha/dt)_{max}$. The t_{max} values of the neat matrix and its composites are mostly comparable. $(d\alpha/dt)_{max}$ of all samples mostly increase with increasing isothermal temperature. Upon heating at 360 °C, $(d\alpha/dt)_{max}$ of HC3 are much lower than those of other samples, indicating that the presence of LCP and carboxylic-functionalized CNT inhibits the decomposition process of polymer matrix. The amounts of char residue for all samples decrease with increasing isothermal temperatures. Note that, under heating at 360 °C, much higher amount of char left is observed for HC3 composite compared among all samples examined.

Evaluation of activation energy for thermo-oxidative decomposition

Nonisothermal activation energy

In general, thermal degradation of polymers usually involves multiple steps that are most likely to have different mechanism and activation energies. The relative

Isothermal activation energy

Generally, for solid-state degradation reaction, the rate of decomposition ($d\alpha/dt$) can be described by [30–32]

$$\frac{d\alpha}{dt} = k(T) f(\alpha) \tag{2}$$

where $k(T)$ represents the reaction rate constant and $f(\alpha)$ is a conversion function. By substituting the Arrhenius equation, $k(T) = A e^{-E_a/RT}$, Eq. (2) becomes
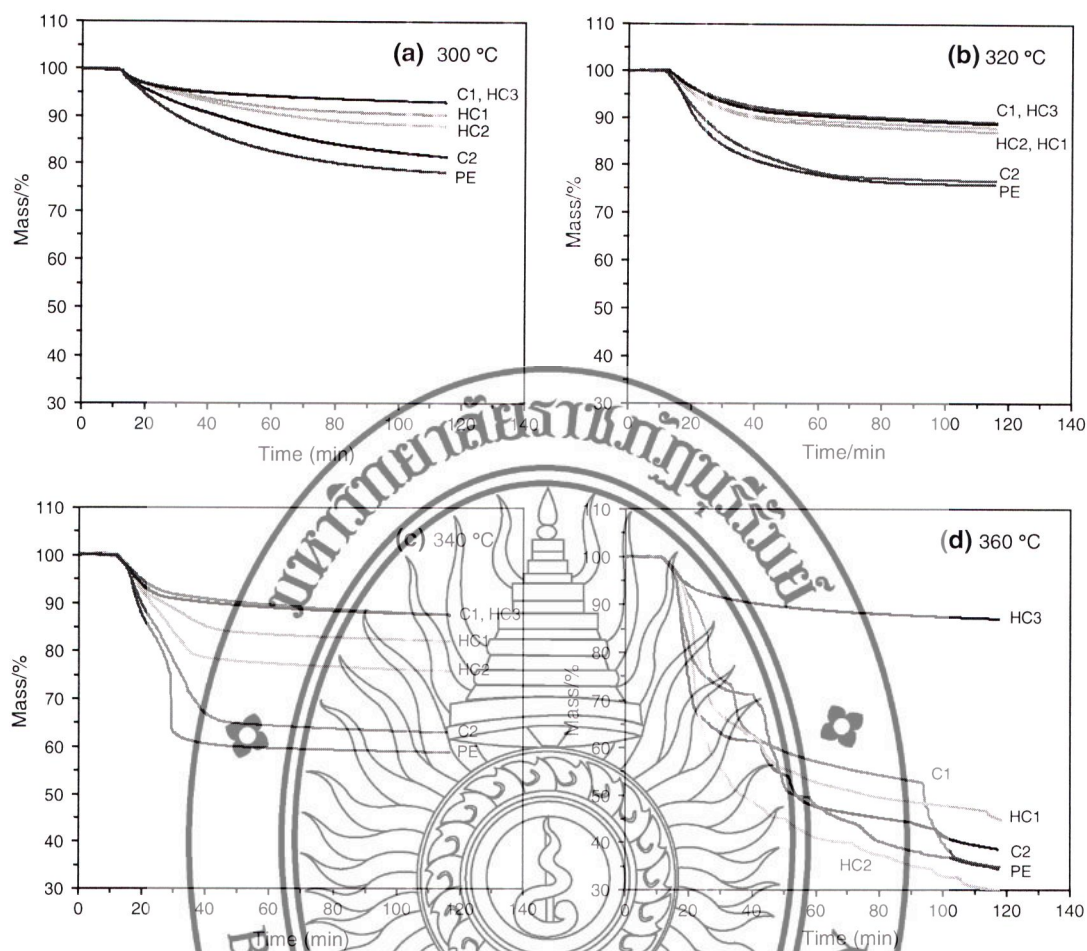
Fig. 4 Isothermal TG curves of PE, C1, C2, HC1, HC2 and HC3 at a 300 °C, b 320 °C, c 340 °C and d 360 °C in air

Table 3 Isothermal decomposition data of PE and its composites

Sample	300 °C			320 °C			340 °C			360 °C		
	$t_{max}/$ min	$(d\alpha/dt)_{max}/$ % min^{-1}	Char yield/%[a]	$t_{max}/$ min	$(d\alpha/dt)_{max}/$ % min^{-1}	Char yield/%[a]	$t_{max}/$ min	$(d\alpha/dt)_{max}/$ % min^{-1}	Char yield/%[a]	$t_{max}/$ min	$(d\alpha/dt)_{max}/$ % min^{-1}	Char yield/%[a]
PE	13.4	0.009	78.2	14.9	0.014	79.2	14.6	0.023	58.7	16.9	0.050	34.6
C1	13.4	0.005	93.0	14.9	0.005	89.1	13.4	0.007	87.7	26.9	0.033	34.9
C2	13.9	0.008	81.8	14.6	0.010	76.6	13.9	0.019	63.0	17.9	0.053	38.7
HC1	13.4	0.006	90.3	15.1	0.007	87.0	13.6	0.012	82.1	25.9	0.023	44.8
HC2	14.3	0.006	87.9	16.3	0.006	87.9	14.7	0.013	75.8	22.9	0.053	29.9
HC3	13.6	0.006	93.1	15.3	0.006	88.8	13.6	0.010	87.5	15.9	0.009	87.2

[a] Char yield is determined after heating for 100 min

$$\frac{d\alpha}{dt} = f(\alpha)\, A e^{-E_a/RT} \quad (3)$$

By the integration of Eq. (3), the integral type of kinetic function, $g(\alpha)$, is obtained:

$$g(\alpha) = A\, e^{-E_a/RT} t \quad (4)$$

where t is a degradation time. By taking the natural logarithm of Eq. (4), the isoconversional equation is derived:
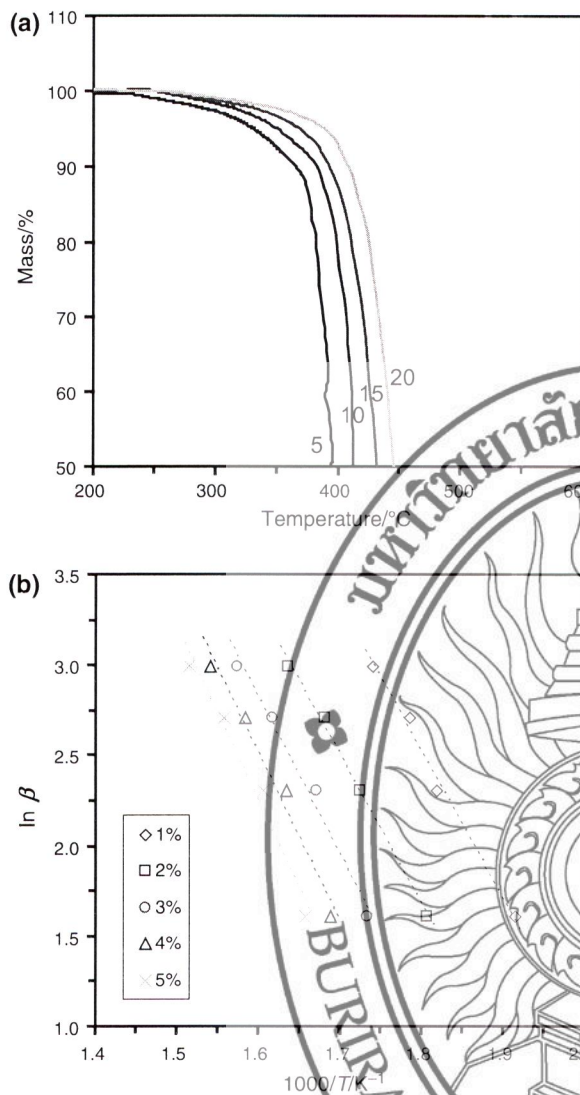
$$\ln t = \ln g(\alpha) - \ln A + \frac{E_a}{RT} \qquad (5)$$

Equation (5) is called standard isoconversional method [33]. The natural logarithm of time t corresponding to a certain mass loss a is linearly dependent on the reciprocal of temperature T. Provided that the order of decomposition reaction n keeps constant within the temperature and mass loss interval under consideration, E_a can be calculated in terms of the slope of the linear relationship of $\ln t$ versus $1/T$. To evaluate the E_a value at a particular mass loss according to the standard isoconversional method, the plot of $\ln t$ versus $1/T$ was investigated. Three straight lines corresponding to the particular mass losses of 3, 5 and 7 mass% for the selected examples, PE and HC3, are illustrated in Fig. 6. The apparent E_a values evaluated from the slopes of the straight lines for the selected samples are listed in Table 5. The results of E_a evaluation from isothermal investigation show the similar trend as those from the nonisothermal one. However, the calculated E_a values are much higher under nonisothermal than under isothermal test.

Melt rheological properties

In this work, the FTIR technique was first employed for study of the interaction between the fillers in the composites. Unfortunately, the useful information could not be gained from the FTIR investigation due to an overlapping of the required peaks. The study on viscoelastic properties using melt rheological measurement is one of the simple techniques widely used for characterization of interaction in the polymer composites or blends. Figure 7 shows the angular frequency (ω) dependence of complex viscosity (η^*) for all analyzed samples. All flow curves exhibit shear thinning behavior; the viscosity decreases with increase in shear rate (or shear frequency). It is seen that, especially at low frequency, the complex viscosities of C1 and C2 are

Fig. 5 Nonisothermal TG curves at heating rates of 5, 10, 15 and 20 °C min⁻¹ (a) and isoconversional plots at particular mass losses of 1, 2, 3, 4 and 5% using W–F–O method (b) for C1 sample

Table 4 Nonisothermal activation energy (E_a) of PE and selected composites in air calculated using Flynn–Wall–Ozawa method

Mass loss/%	E_a (r^*)/kJ mol⁻¹			
	PE	C1	HC1	HC3
1	79.4 (0.9669)	69.1 (0.9902)	65.6 (0.9998)	68.9 (0.9613)
2	71.4 (0.9829)	70.6 (0.9963)	68.2 (0.9910)	70.6 (0.9730)
3	75.7 (0.9856)	74.1 (0.9840)	71.1 (0.9667)	85.1 (0.9680)
4	85.5 (0.9665)	78.9 (0.9766)	74.3 (0.9613)	99.9 (0.9940)
5	89.4 (0.9822)	81.5 (0.9827)	80.9 (0.9723)	101 (0.9871)
Average	80.8	74.8	72.0	85.2

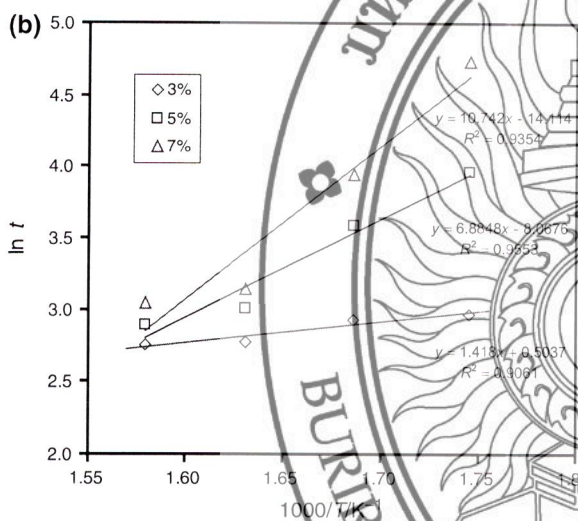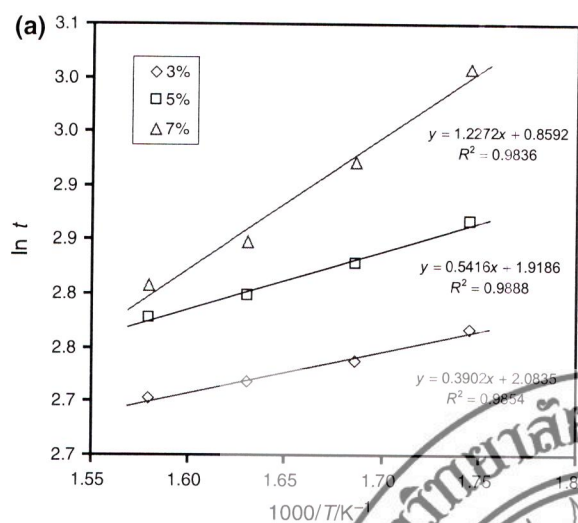* r means the correlation for the linear fit analysis

Fig. 6 Application of standard isoconversional method to the thermo-oxidative degradation of PE (**a**) and HC3 (**b**) at particular mass losses of 3, 5 and 7%

comparable and slightly higher than that of the neat matrix. In case of LCP-containing composite (C1), the presence of LCP normally lowers the melt viscosity of the composite system. However, as reported previously [34], the LCP can be clearly functioned as the lubricating agent under loading with high content (>10 mass%). It is seen that the further increase in the melt viscosity is observed for the hybrid composites. In particular for HC3, the complex viscosity at low frequency shows the highest value. The obtained results clearly indicated the effective interaction between the LCP and carboxylic-functionalized CNT for the HC3
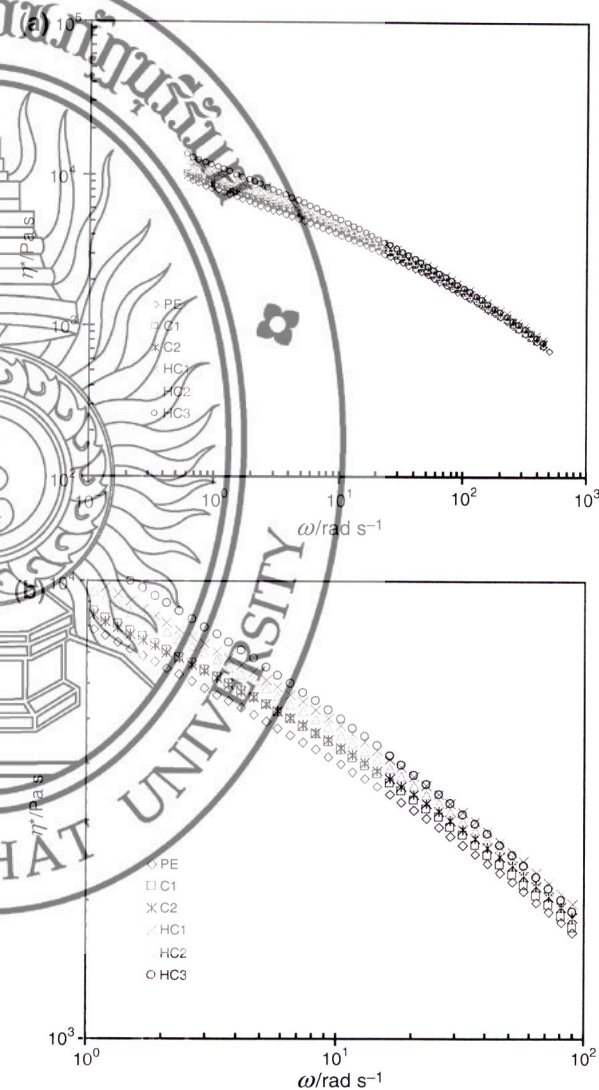
Table 5 Activation energy (E_a) for isothermal degradation of PE and selected composites in air calculated using standard isoconversional method

Mass loss/%	E_a (r^*)/kJ mol^{-1}			
	PE	C1	HC1	HC3
3	3.24 (0.9854)	12.8 (0.9196)	3.40	11.8 (0.9061)
5	4.50 (0.9888)	44.5 (0.9195)	25.1	57.2 (0.9553)
7	10.2 (0.9856)	82.5 (0.9705)	45.5	89.3 (0.9354)
Average	5.98	46.6	24.7	52.8

* r means the correlation for the linear fit analysis

Fig. 7 Plots of complex viscosity as a function of angular frequency (**a**) and expanded region from 1 to 100 rad s^{-1} (**b**) for polyethylene and its composites at 225 °C

sample. It is interesting to note that, at high frequency, the melt flow curve of each sample is converged together and the viscosity values are nearly the same. This means that the effects of filler loadings and interaction between the fillers cannot be prolonged under melt flow state at high shear force (frequency). These results agree well with the PET/CNT nanocomposites reported by Jin et al. [35]. They report that effect of functionalized CNT in melt viscosity is mostly pronounced at low frequency and the relative effect diminishes with increasing frequency. Moreover, they found that the melt viscosity of PET/diamine CNT is clearly higher than that of the PET/pristine CNT composites due to the partial cross-linking between PET and functionalized CNT.

The elastic and viscous characteristics of both blend systems can be considered from the plots of storage modulus (G') and loss modulus (G''), respectively, as a function of ω. The plots of G' and G'' as a function of ω for the neat matrix and its composites are shown in Fig. 8. The values of G' and G'' at low frequency generally provide information about long-range (beyond entanglement distance) relaxation, while the values at high frequency provide information about short-range (motion with entanglement) relaxation [36]. It is seen that G' and G'' of all samples increase with increasing frequency, indicating a viscoelastic properties dependence of the timescale of molecular motion. Moreover, G'' value of each polymer is higher than G' in the frequency range of 0.6–100 rad s^{-1}, indicating that the viscous property is a dominant factor. As seen from the expanded curves in Fig. 8b, it is clearly seen that HC3 shows the highest G' and G'' values, whereas the neat polymer matrix shows lowest viscoelastic values. This indicates that the presence of fillers in the polymer matrix with forming filler–filler interaction plays an important role in hindering the chain mobility, leading to an increase in chain rigidity. It should be noted that the hybrid composites (HC1, HC2 and HC3) exhibit higher viscoelastic value compared to the ordinary (binary components) composites (C1 and C2). Moreover, the crossing of G' and G'' curves is observed at frequency higher than 100 rad s^{-1}, indicating that the elastic properties of all samples are pronounced at high frequency.

Morphology

Figure 9 shows the SEM (column I) and TEM (column II) images of the composites. For SEM images, the composites with the presence of LCP (C1, HC1, HC2 and HC3) clearly show the droplets morphology of LCP phase with the diameter of 0.5–3 μm. The relatively lower diameter of LCP droplets is clearly observed for HC3. In case of TEM images, the pullout trace of LCP domains is clearly
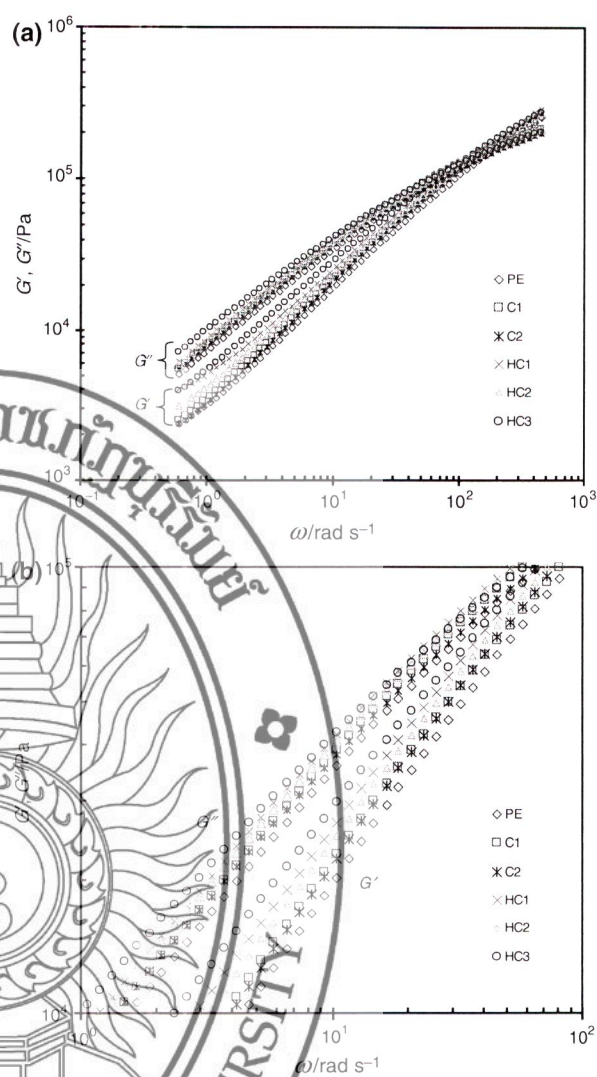

Fig. 8 Plots of storage (G') and loss (G'') modulus as a function of angular frequency (a) and the expanded plots in the region from 1 to 100 rad s^{-1} (b) for polyethylene and its composites at 225 °C

observed for C1 composite as seen from Fig. 9II-a (see arrows). The pullout effect for LCP is mostly observed for all LCP-containing composite systems resulting from the ultracutting process during the sample preparation for TEM analysis. For C2, the aggregation with poor dispersion state of the pristine CNT is observed (see arrows in Fig. 9II-b). In case of the hybrid composites, the morphology of the nanotubes is focused. The nonuniform dispersion of the nanotubes in HC1 and HC2 is clearly found as seen from Fig. 9II-c, II-d. Better dispersion of the nanotube aggregates compared to other composites is observed for HC3 (Fig. 9II-e). Moreover, the TEM image at the LCP/CNT-COOH interface is observed as seen in Fig. 10a. It is

Fig. 9 SEM (*column I*) and TEM (*column I*) images for **a** C1, **b** C2, **c** HC1, **d** HC2 and **e** HC3

clearly seen that some part of the CNT-COOH is adhered on the LCP surface indicating the presence of interaction at the interface. Based on the morphological results, the proposed dispersion states of CNTs and LCP in the PE-based composites with and without the presence of interface interaction can be schematically drawn as shown in Fig. 10b, c. As known that LCP can be immiscibly dispersed in the thermoplastics during melt mixing. Therefore, the better dispersion of LCP interacted with carboxylic-functionalized CNT through hydrogen bonding would assist the dispersion of the nanotube [25]. Moreover, the interfacial bonding between the functionalized nanotubes and LCP would improve the LCP domains as seen from Fig. 9I-e.
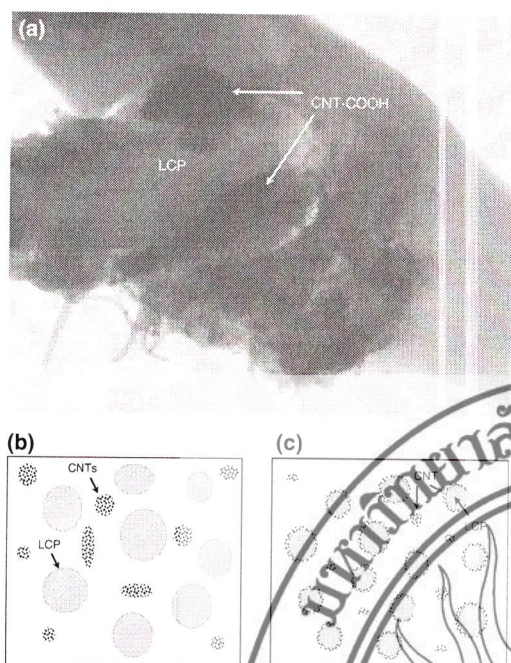
Fig. 10 TEM image at LCP/CNT-COOH interface for HC3 (a) and proposed dispersion states of CNT and LCP with the absence (b) and presence (c) of LCP/CNT interaction

Conclusions

This study investigated the effect of LCP and CNTs fillers on thermo-oxidative stability of PE-based thermoplastic composites. For nanofillers, hydroxyl- and carboxylic-functionalized CNTs were used in comparison with the pristine one. Among all samples examined, the hybrid composite containing carboxylic-functionalized CNT (HC3) exhibited the highest thermo-oxidative stability under applied dynamic and isothermal modes of heating. The highest melt viscosity of HC3 revealed from rheological measurements indicated the presence of good interaction between LCP and carboxylic-functionalized CNT. The morphological studies indicated the improved dispersion of both LCP and carboxylic-functionalized CNT fillers as a result from the presence of interface interaction. The present findings suggested the important role of LCP-assisted CNT dispersion by forming interaction at the interface, resulting in the significant improvement in thermo-oxidative stability of the composite material.

References

1. Acierno D, Collyer AA. Rheology and processing of liquid crystal polymers. Polymer liquid crystal series, vol. 2. 1st ed. London: Chapman & Hall; 1996.
2. Tjong S. Structure, morphology, mechanical and thermal characteristics of the in situ composites based on liquid crystalline polymer and thermoplastics. Mater Sci Eng. 2003;R41:1–60.
3. Kiss G. In situ composites: blends of isotropic polymers and thermotropic liquid crystalline polymers. Polym Eng Sci. 1987;27:410–23.
4. Kim JY, Kim SH. Influence of viscosity ratio on processing and morphology of thermotropic liquid crystal polymer-reinforced poly(ethylene 2,6-naphthalate) blends. Polym Int. 2006;55:449–55.
5. Kim JY, Kim SH. Structure and property relationship of thermotropic liquid crystal polymer and polyester composite fibers. J Appl Polym Sci. 2006;99:2211–9.
6. Kim JY, Kim SH. In Situ fibril formation of thermotropic liquid crystal polymer in polyesters blends. J Polym Sci, Part B: Polym Phys. 2005;43:3600–10.
7. Ren P-G, Si XH, Sun Z-F, Ren F, Pei L, Hou S-Y. Synergistic effect of BN and MWCNT hybrid fillers on thermal conductivity and thermal stability of ultra-high-molecular-weight polyethylene composites with a segregated structure. J Polym Res. 2016;23:21.
8. Saengsuwan S, Saikrasun S. Thermal stability of styrene–(ethylene butylene)–styrene-based elastomer composites modified by liquid crystalline polymer, clay, and carbon nanotube. J Therm Anal Calorim. 2012;110:1395–406.
9. Xie XL, Mai YW, Zhou XP. Dispersion and alignment of carbon nanotubes in polymer matrix: a review. Mater Sci Eng R Rep. 2005;49:89–112.
10. Yang SY, Castilleja JR, Barrera EV, Lozano K. Thermal analysis of an acrylonitrile–butadiene–styrene/SWNT composite. Polym Degrad Stab. 2004;83:383–8.
11. Probst O, Moore EM, Resasco DE, Grady BP. Nucleation of polyvinyl alcohol crystallization by single-walled carbon nanotubes. Polymer. 2004;45:4437–43.
12. Kashiwagi T, Grulke E, Hilding J, Harris R, Awad W, Douglas J. Thermal degradation and flammability properties of poly(propylene)/carbon nanotubes composites. Macromol Rapid Commun. 2002;23:761–5.
13. Cheng HKF, Chong MF, Liu E, Zhou K, Li L. Thermal decomposition kinetics of multiwalled carbon nanotube/polypropylene nanocomposites. J Therm Anal Calorim. 2014;117:63–71.
14. Liu J, Rinzler AG, Dai H, Hafner JH, Bradley RK, Boul PJ, Lu A, Iverson T, Shelimov K, Huffman CB, Rodriguez-Macias F, Shon Y-S, Lee TR, Colbert DT, Smalley RE. Fullerene pipes. Science. 1998;280:1253–6.
15. Sun Y-P, Fu K, Lin Y, Huang W. Functionalized carbon nanotubes: properties and applications. Acc Chem Res. 2002;35:1096–104.
16. Müller MT, Pötschke P, Voit B. Dispersion of carbon nanotubes into polyethylene by an additive assisted one-step melt mixing approach. Polymer. 2015;66:210–21.
17. Prashantha K, Soulestin J, Lacrampe MF, Krawczak P, Dupin G, Claes M. Masterbatch-based multi-walled carbon nanotube filled polypropylene nanocomposites: assessment of rheological and mechanical properties. Compos Sci Technol. 2009;69:1756–63.
18. Xu D, Wang Z. Role of multi-wall carbon nanotube network in composites to crystallization of isotactic polypropylene matrix. Polymer. 2008;49:330–8.
19. Yang B-X, Pramoda KP, Xu GQ, Goh SH. Mechanical reinforcement of polyethylene using polyethylene-grafted multi-walled carbon nanotubes. Adv Funct Mater. 2007;17:2062–9.

20. Vega JF, Martínez-Salazar J, Trujillo M, Arnal ML, Müller AJ, Bredeau S, Dubois PH. Rheology, processing, tensile properties, and crystallization of polyethylene/carbon nanotube nanocomposites. Macromolecules. 2009;42:4719–27.

21. Cheng HKF, Pan Y, Sahoo NG, Chong K, Li L, Chan SH, Zhao J. Improvement in properties of multiwalled carbon nanotube/polypropylene nanocomposites through homogeneous dispersion with the aid of surfactants. J Appl Polym Sci. 2012;124:1117–27.

22. Jin SH, Kang CH, Yoon KH, Bang DS, Park YB. Effect of compatibilizer on morphology, thermal, and rheological properties of polypropylene/functionalized multi-walled carbon nanotubes composite. J Appl Polym Sci. 2009;111:1028–33.

23. Lee SH, Cho E, Jeon SH, Youn JR. Rheological and electrical properties of polypropylene composites containing functionalized multi-walled carbon nanotubes and compatibilizers. Carbon. 2007;45:2810–22.

24. Wu D, Sun Y, Zhang M. Kinetics study on melt compounding of carbon nanotube/polypropylene nanocomposites. J Polym Sci, Part B: Polym Phys. 2009;47:608–18.

25. Kim JY, Kim DK, Kim SH. Effect of modified carbon nanotube on physical properties of thermotropic liquid crystal polyester nanocomposites. Euro Polym J. 2009;45:316–24.

26. Peterson JD, Vyazovkin S, Wight C. Kinetics of thermal and thermo-oxidative degradation of polystyrene, polyethylene and poly(propylene). Macromol Chem Phys. 2001;202:775–84.

27. Chrissafis K, Bikiaris D. Can nanoparticles really enhance thermal stability of polymers? Part I: an overview on thermal decomposition of addition polymers. Thermochim Acta. 2011; 523:1–24.

28. Ozawa T. A new method of analyzing thermogravimetric data. Bull Chem Soc Jpn. 1965;38:1881.

29. Flynn JH, Wall LA. General treatment of the thermogravimetry of polymers. J Res Natl Bur Stds. 1966;70A:487–523.

30. Hatakeyama T, Quinn FX. Thermal analysis: fundamentals and applications to polymer science. 2nd ed. Chichester: Wiley; 1999.

31. Nam JD, Seferis JC. A composite methodology for multistage degradation of Polymers. J Polym Sci B Polym Phys. 1991; 29:601–8.

32. Vyazovkin S, Wight CA. Isothermal and nonisothermal reaction kinetics in solids: in search of ways toward consensus. J Phys Chem. 1997;101:8279–84.

33. Vyazovkin S. Computational aspects of kinetic analysis.: part C. The ICTAC kinetics project—the light at the end of the tunnel? Thermochim Acta. 2000;355:155–63.

34. Kayaisang S, Amornsakchai T, Saikrasun S. Influence of liquid crystalline polymer and recycled PET as minor blending components on rheological behavior, morphology, and thermal properties of thermoplastic blends. Polym Adv Technol. 2009; 20:1136–45.

35. Jin SH, Park YB, Yoon KH. Rheological and mechanical properties of surface modified multi-walled carbon nanotube-filled PET composite. Compos Sci Technol. 2007;67:3434–41.

36. Hsieh TT, Tiu C, Hsieh KH, Simon GP. Characterization of thermotropic liquid crystalline polyester/polycarbonate blends: miscibility, rheology, and free volume behavior. J Appl Polym Sci. 2000;77:2319–30.